



Radiative neutrino masses.

Antonio Enrique Cárcamo Hernández

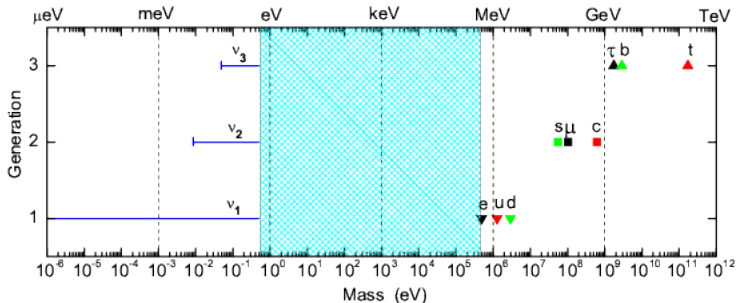
Departamento de Física, Universidad Técnica Federico Santa María
Centro Científico-Tecnológico de Valparaíso, Casilla 110-V, Valparaíso, Chile
Millennium Institute for Subatomic Physics at the High-Energy Frontier, SAPHIR, Chile

8th International Conference of High Energy Physics at the LHC Era,
Valparaíso, Chile, 10th January of 2023.

Based on: AECH, C. Hati, S. Kovalenko, J. W. F. Valle and
C. A. Vaquera-Araujo, JHEP **03**, 034 (2022)

A. Abada, N. Bernal, AECH, S. Kovalenko, T. B. de Melo and
T. Toma, arXiv:2212.06852.

Introduction

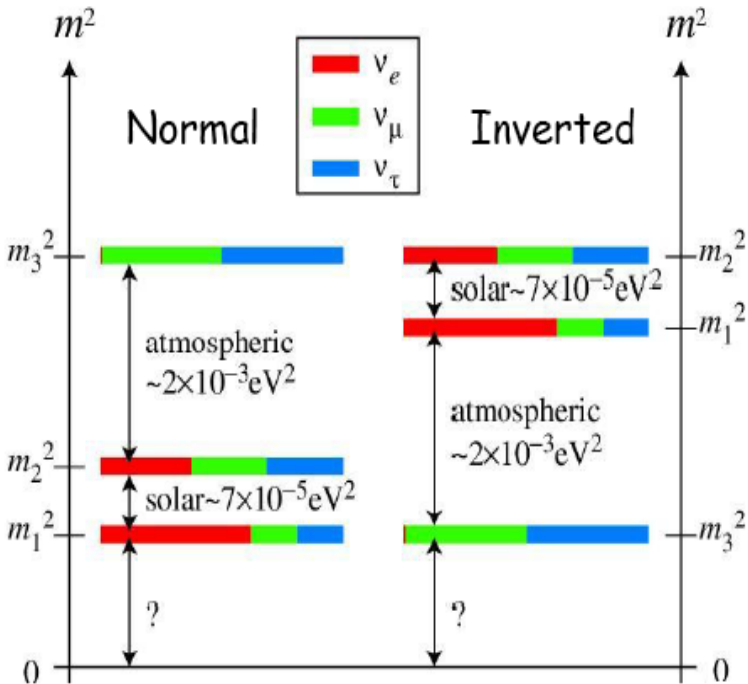


CKM

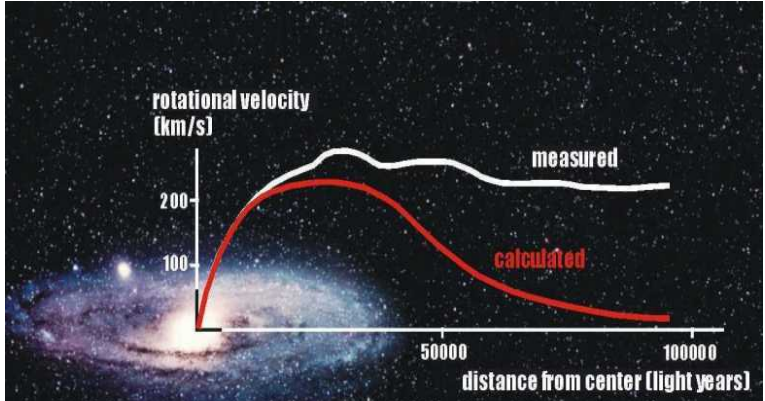
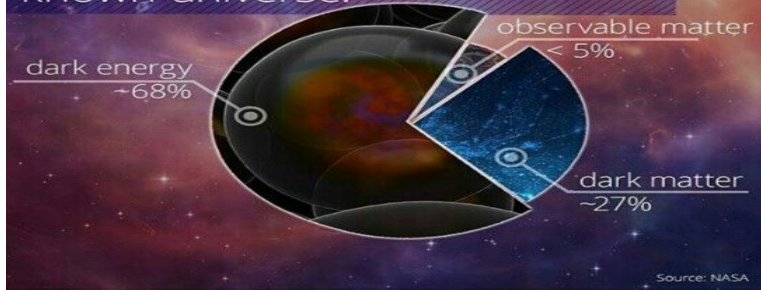
$$|V| = \begin{matrix} & d & s & b \\ \begin{matrix} u \\ c \\ t \end{matrix} & \begin{bmatrix} \text{orange} & \text{green} & \cdot \\ \text{green} & \text{orange} & \text{blue} \\ \cdot & \text{blue} & \text{orange} \end{bmatrix} \end{matrix}$$

PMNS

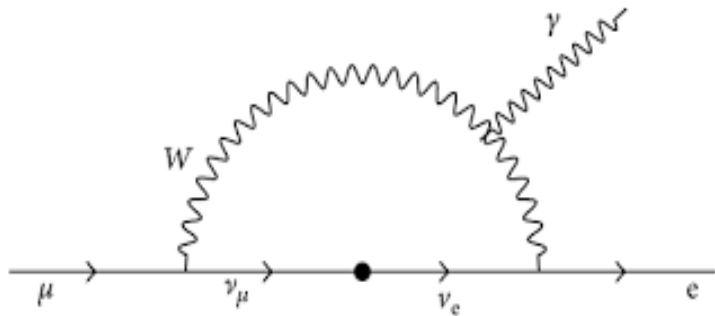
$$|U| = \begin{matrix} & 1 & 2 & 3 \\ \begin{matrix} e \\ \mu \\ \tau \end{matrix} & \begin{bmatrix} \text{orange} & \text{green} & \text{black} \\ \text{green} & \text{orange} & \text{blue} \\ \text{black} & \text{blue} & \text{orange} \end{bmatrix} \end{matrix}$$

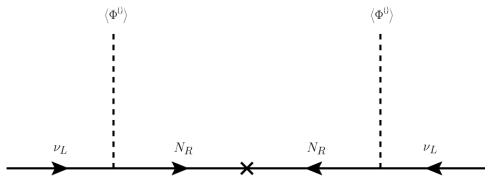


known universe:



$$Br_{SM}(\mu \rightarrow e\gamma) \sim \mathcal{O}(10^{-54}), \quad Br_{exp}(\mu \rightarrow e\gamma) < 4.2 \times 10^{-13}$$





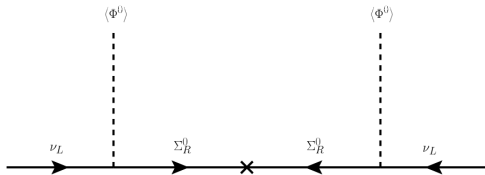
Type I seesaw

$$LHN \quad 2 \otimes 2 \otimes 1$$

Minkowski 1977, Gellman, Ramond, Slansky 1980

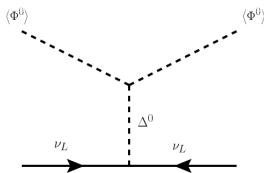
Glashow, Yanagida 1979, Mohapatra, Senjanovic 1980

Lazarides Shafi Weterrich 1981, Schechter-Valle 1980 and 1982



Type III seesaw

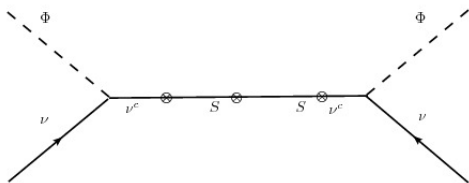
$$LH\Sigma \quad 2 \otimes 2 \otimes 3$$



Type II seesaw

$$L\Delta L \quad 2 \otimes 3 \otimes 2$$

Schechter-Valle 1980 and 1982



Inverse seesaw

$$-\mathcal{L}_{mass}^{(\nu)} = \frac{1}{2} \begin{pmatrix} \overline{\nu_L^c} & \overline{N_R} & \overline{S_R} \end{pmatrix} \mathbf{M}_\nu \begin{pmatrix} \nu_L \\ N_R^c \\ S_R^c \end{pmatrix} + H.c$$

$$\mathbf{M}_\nu = \begin{pmatrix} 0_{3 \times 3} & \mathbf{M}_1 & \mathbf{M}_L \\ \mathbf{M}_1^T & 0_{3 \times 3} & \mathbf{M}_2 \\ \mathbf{M}_L^T & \mathbf{M}_2^T & \mu \end{pmatrix}$$

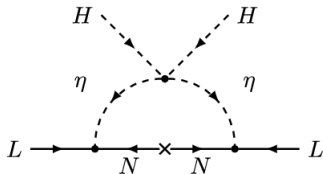
$$\mathbf{M}_L = 0_{3 \times 3}$$

$$Q_{\nu_L}^{U(1)_L} = Q_{S_R}^{U(1)_L} = -Q_{N_R}^{U(1)_L} = 1$$

$$\tilde{\mathbf{M}}_\nu = \mathbf{M}_1 (\mathbf{M}_2^T)^{-1} \mu \mathbf{M}_2^{-1} \mathbf{M}_1^T$$

$$\mathbf{M}_\nu^{(1)} = -\frac{1}{2} (\mathbf{M}_2 + \mathbf{M}_2^T) + \frac{1}{2} \mu$$

$$\mathbf{M}_\nu^{(2)} = \frac{1}{2} (\mathbf{M}_2 + \mathbf{M}_2^T) + \frac{1}{2} \mu$$



One loop Ma radiative seesaw model

η and N are odd under a preserved Z_2

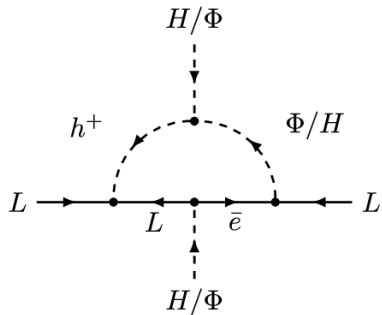
$$L \tilde{\eta} N, \frac{\lambda_5}{2} (H^\dagger \cdot \eta)^2 + h.c$$



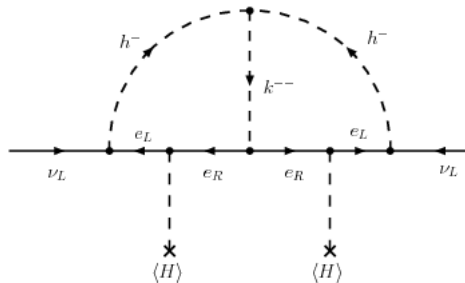
Linear seesaw:

$$\mu = 0_{3 \times 3}$$

$$\tilde{\mathbf{M}}_\nu = -\mathbf{M}_L \mathbf{M}_2^{-1} \mathbf{M}_1^T - \mathbf{M}_1 (\mathbf{M}_2^T)^{-1} \mathbf{M}_L^T$$

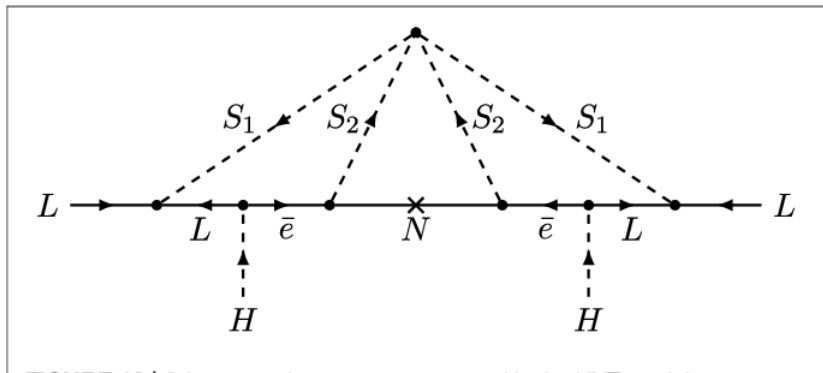


Zee model

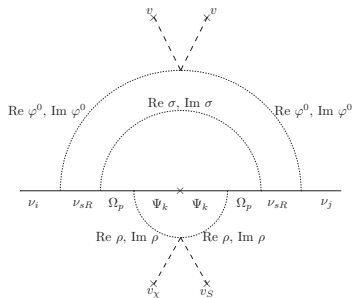
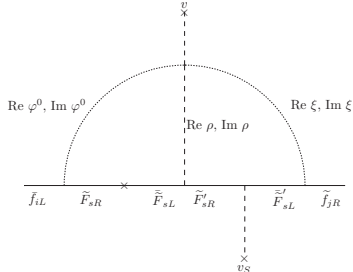
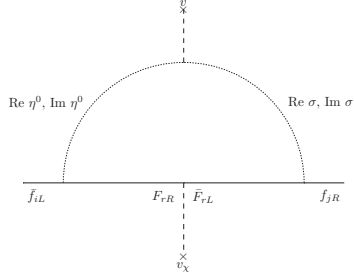


Zee Babu model

Field	Spin	G_{SM}	Z_2
S_1	0	$(1, 1, -1)$	+
S_2	0	$(1, 1, -1)$	-
N	$\frac{1}{2}$	$(1, 1, 0)$	-



KNT model



$$m_\nu \sim l^3 y^6 \lambda \frac{v^2}{M},$$

$$y \sim 0.3, \lambda \sim 0.1$$

$$M \sim \mathcal{O}(13) \text{ TeV}$$

$$m_\nu \sim \mathcal{O}(0.1) \text{ eV}$$

AECH, S. Kovalenko, M. Maniatis and I. Schmidt, "Fermion mass hierarchy and $g - 2$ anomalies in an extended 3HDM Model," JHEP **10** (2021), 036

Scotogenic neutrino masses with GCU

Field	SU(3) _c	SU(3) _L	U(1) _X	U(1) _N	Q	$M_P = (-1)^{3(B-L)+2s}$
q_{iL}	3	$\bar{\mathbf{3}}$	0	0	$(-\frac{1}{3}, \frac{2}{3}, -\frac{1}{3})^T$	$(++-)^T$
q_{3L}	3	3	$\frac{1}{3}$	$\frac{2}{3}$	$(\frac{2}{3}, -\frac{1}{3}, \frac{2}{3})^T$	$(++-)^T$
u_{aR}	3	1	$\frac{2}{3}$	$\frac{1}{3}$	$\frac{2}{3}$	+
d_{aR}	3	1	$-\frac{1}{3}$	$\frac{1}{3}$	$-\frac{1}{3}$	+
U_{3R}	3	1	$\frac{2}{3}$	$\frac{4}{3}$	$\frac{2}{3}$	-
D_{iR}	3	1	$-\frac{1}{3}$	$-\frac{2}{3}$	$-\frac{1}{3}$	-
l_{aL}	1	3	$-\frac{1}{3}$	$-\frac{2}{3}$	$(0, -1, 0)^T$	$(++-)^T$
e_{aR}	1	1	-1	-1	-1	+
ν_{iR}	1	1	0	-4	0	-
ν_{3R}	1	1	0	5	0	+
Ω_{aL}	1	8	0	0	$\begin{pmatrix} 0 & 1 & 0 \\ -1 & 0 & -1 \\ 0 & 1 & 0 \end{pmatrix}$	$\begin{pmatrix} - & - & + \\ - & - & + \\ + & + & - \end{pmatrix}$
η	1	3	$-\frac{1}{3}$	$\frac{1}{3}$	$(0, -1, 0)^T$	$(++-)^T$
ρ	1	3	$\frac{2}{3}$	$\frac{1}{3}$	$(1, 0, 1)^T$	$(++-)^T$
χ	1	3	$-\frac{1}{3}$	$-\frac{2}{3}$	$(0, -1, 0)^T$	$(--+)^T$
ϕ	1	1	0	2	0	+
σ	1	1	0	1	0	-

Table: 3311 model field content ($a = 1, 2, 3$ and $i = 1, 2$ are family indices).

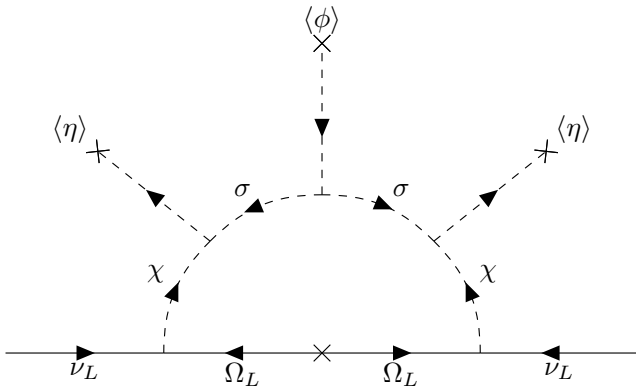


Figure: Feynman-loop diagram contributing to the light active Majorana neutrino mass matrix.

In the limit where the trilinear scalar interactions $\phi^+\sigma^2$ and $(\eta^+\chi)\sigma$ are absent, the model Lagrangian has an accidental $U(1)$ symmetry under which ϕ and σ have the same charge whereas the remaining fields are neutral under this symmetry.

$$Q = T_3 - \frac{T_8}{\sqrt{3}} + X, \quad B - L = -\frac{2}{\sqrt{3}}T_8 + N, \quad (1)$$

$$q_{iL} = \begin{pmatrix} d_i \\ -u_i \\ D_i \end{pmatrix}_L, \quad q_{3L} = \begin{pmatrix} u_3 \\ d_3 \\ U_3 \end{pmatrix}_L, \quad l_{aL} = \begin{pmatrix} \nu_a \\ e_a \\ N_a \end{pmatrix}_L, \quad (2)$$

The gauged $B - L$ symmetry is spontaneously broken leaving a discrete remnant symmetry $M_P = (-1)^{3(B-L)+2s}$.

$$\begin{aligned} \langle \eta \rangle &= \frac{1}{\sqrt{2}}(v_1, 0, 0)^T, & \langle \rho \rangle &= \frac{1}{\sqrt{2}}(0, v_2, 0)^T, & \langle \chi \rangle &= (0, 0, w)^T, \\ \langle \phi \rangle &= \frac{1}{\sqrt{2}}\Lambda, & \langle \sigma \rangle &= 0. \end{aligned} \quad (3)$$

We assume $w, \Lambda, \gg v_1, v_2$, such that the SSB pattern of the model is

$$\begin{aligned} &SU(3)_C \times SU(3)_L \times U(1)_X \times U(1)_N \\ &\quad \downarrow w, \Lambda \\ &SU(3)_C \times SU(2)_L \times U(1)_Y \times M_P \\ &\quad \downarrow v_1, v_2 \\ &SU(3)_C \times U(1)_Q \times M_P. \end{aligned} \quad (4)$$

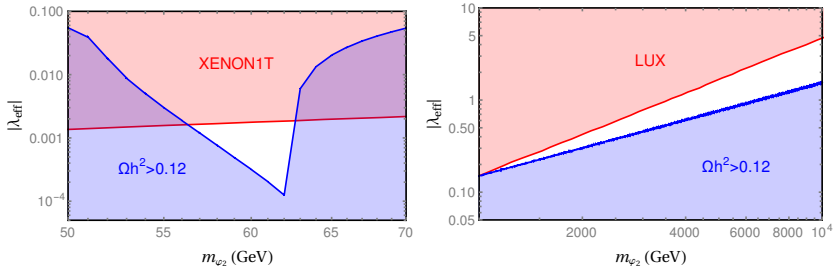


Figure: Viable mass regions where the field φ_2 of the simplified model described in the text behaves as a dark matter candidate. The red regions correspond to the current direct detection limits. The blue regions represent values of the effective coupling λ_{eff} where the corresponding relic density is incompatible with the Planck measurement.

For the case of fermionic DM candidate, one has:

$$\langle \sigma v \rangle \approx \left(\frac{\alpha}{150 \text{ GeV}} \right)^2 \left(\frac{M_\Omega}{3 \text{ TeV}} \right)^2 \approx \left(\frac{M_\Omega}{3 \text{ TeV}} \right)^2 \text{ pb}, \quad (5)$$

$$\Omega_{DM} h^2 = \frac{0.1 \text{ pb}}{\langle \sigma v \rangle}, \quad (6)$$

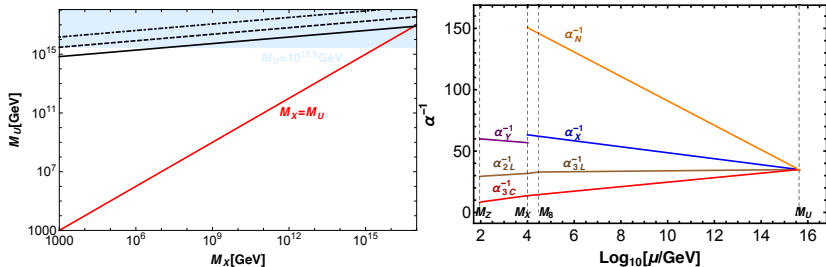


Figure: Left) Unification scale M_U as a function of the 3-3-1-1 symmetry breaking scale M_X , for three benchmark choices $M_8 = M_X$ (solid curve), $M_8 = 3M_X$ (dashed curve) and $M_8 = 10M_X$ (dot-dashed curve). (Right) An example of $SU(3)_c \times SU(3)_L \times U(1)_X \times U(1)_N$ unification for a phenomenologically accessible 3-3-1-1 symmetry breaking scale $M_X = 10 \text{ TeV}$ and $M_8 = 3M_X = 30 \text{ TeV}$.

Scotogenic three-loop neutrino mass model

Field	q_{iL}	u_{iR}	d_{iR}	l_{iL}	l_{iR}	N_{R_k}	ϕ	η	φ	ρ	ζ	σ
$SU(3)_C$	3	3	3	1	1	1	1	1	1	1	1	1
$SU(2)_L$	2	1	1	2	1	1	2	2	1	1	1	1
$U(1)_Y$	$\frac{1}{6}$	$\frac{2}{3}$	$-\frac{1}{3}$	$-\frac{1}{2}$	-1	0	$\frac{1}{2}$	$\frac{1}{2}$	0	0	0	0
$U(1)'$	$\frac{1}{3}$	$\frac{1}{3}$	$\frac{1}{3}$	-3	-3	0	0	3	3	-1	0	$\frac{1}{2}$
\mathbb{Z}_2	1	1	1	1	1	-1	1	-1	-1	-1	-1	1

Table: Particle charge assignments under the $SU(3)_C \otimes SU(2)_L \otimes U(1)_Y \otimes U(1)' \otimes \mathbb{Z}_2$ symmetry. Here $i = 1, 2, 3$ and $k = 1, 2$.

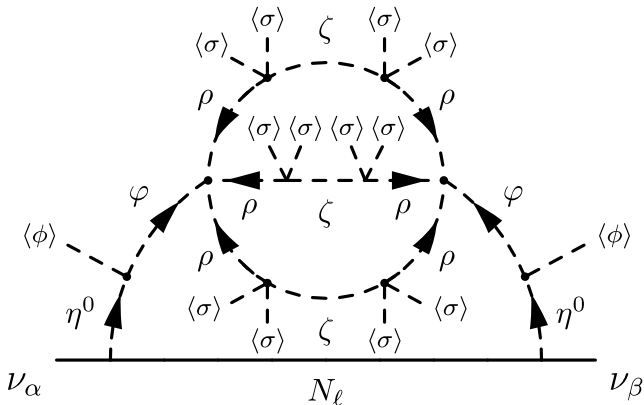


Figure: Scotogenic loop for light active neutrino masses where $\ell = 1, 2$ and $\alpha, \beta = e, \mu, \tau$. The scalar quartic coupling $(\phi^\dagger \eta)^2$ arises at two-loop level. In the limit where the trilinear scalar interaction $A [(\eta^\dagger \phi) \phi + \text{H.c.}]$ is absent, the model Lagrangian has an accidental $U(1)_X$ symmetry under which the inert $SU(2)_L$ scalar doublet η has charge -1 and the charges of the left and right leptonic fields are equal to 1, while the remaining fields are neutral.

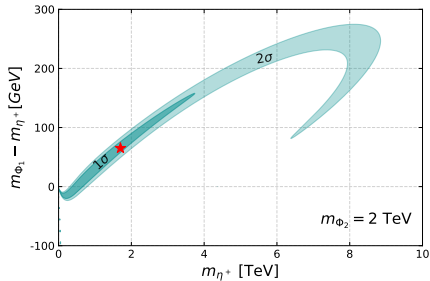
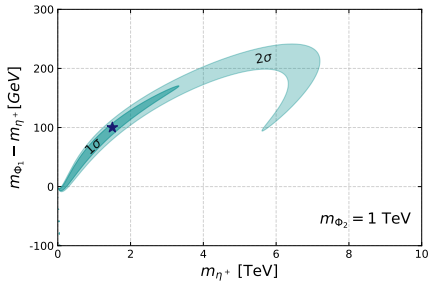


Figure: The $1\text{-}\sigma$ and $2\text{-}\sigma$ regions in the $m_{\Phi_1} - m_{\eta^+}$ versus m_{η^+} plane allowed by the fit of the oblique S , T and U parameters including the CDF measurement of the W mass. In the left (right) panel the mass of the neutral scalar Φ_2 is $m_{\Phi_2} = 1$ TeV ($m_{\Phi_2} = 2$ TeV). In both cases, the mixing angle is fixed at $\theta_{\Phi} = 0.2$.

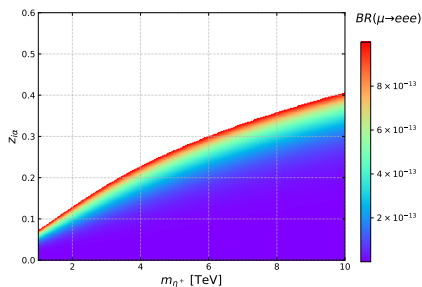
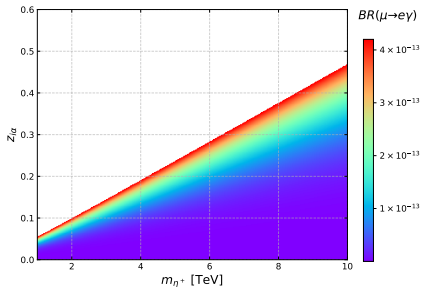
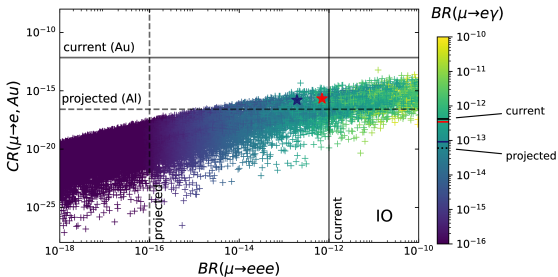
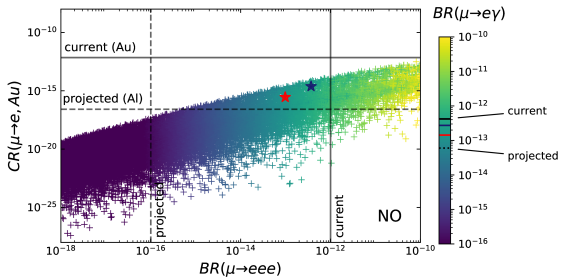


Figure: Parameter space in the $m_{\eta^+} - z_{i\alpha}$ plane consistent with the charged lepton flavor violation limits. The colored regions are allowed by the current constraints.



- Dark matter stability can arise from a residual matter-parity symmetry.
- Leptonic $SU(3)_L$ octets allow GCU and one loop scotogenic neutrino generation. DM can also be accounted for.
- Tiny active neutrino masses can be generated at three loop level within a minimal extended IDM.
- The minimal extended IDM accommodates oblique parameter constraints, W mass anomaly and leads to CLFV processes within the reach of the future experimental sensitivity.

Acknowledgements

Thank you very much to all of you for the attention.

A.E.C.H was supported by Fondecyt (Chile), Grant No. 1210378 and ANID- Programa Milenio - code ICN2019_044.

Extra Slides

$$\begin{pmatrix} \eta^0 \\ \varphi \end{pmatrix} = \begin{pmatrix} \cos \theta_\Phi & \sin \theta_\Phi \\ -\sin \theta_\Phi & \cos \theta_\Phi \end{pmatrix} \begin{pmatrix} \Phi_1 \\ \Phi_2 \end{pmatrix}, \quad (7)$$

$$\begin{pmatrix} \rho_R \\ \zeta_R \end{pmatrix} = \begin{pmatrix} \cos \theta_{\Xi} & \sin \theta_{\Xi} \\ -\sin \theta_{\Xi} & \cos \theta_{\Xi} \end{pmatrix} \begin{pmatrix} \Xi_1 \\ \Xi_2 \end{pmatrix}, \quad (8)$$

$$\begin{pmatrix} \rho_l \\ \zeta_l \end{pmatrix} = \begin{pmatrix} \cos \theta'_{\Xi} & \sin \theta'_{\Xi} \\ -\sin \theta'_{\Xi} & \cos \theta'_{\Xi} \end{pmatrix} \begin{pmatrix} \Xi_3 \\ \Xi_4 \end{pmatrix}. \quad (9)$$

Parameters	Scanned ranges
θ_R	$[0, 2\pi]$
λ_{14}	$[0.01, 1]$
$m_{N_R}, m_{\eta^+}, m_{\Phi_{1,2}}, m_{\Xi_{1,2,3,4}}$	$[500, 10000]$ GeV

Table: Scanned parameter ranges.

θ_Φ	0.2		0.2	
θ_Ξ	0.3		0.3	
θ'_Ξ	0.1		0.1	
m_{η^+} [GeV]	1500		1700	
m_{Φ_1} [GeV]	1600		1765	
m_{Φ_2} [GeV]	1000		2000	
m_{N_R} [GeV]	8954.5	4246.9	5040.0	3450.7
m_{Ξ_1} [GeV]	8130.4	2925.0	8244.0	3282.9
m_{Ξ_2} [GeV]	1452.5	4748.5	2431.6	1815.4
m_{Ξ_3} [GeV]	8932.4	2763.1	6392.1	3637.6
m_{Ξ_4} [GeV]	7127.2	9336.4	1296.0	1458.4
λ_{14}	0.729	0.726	0.363	0.504
y_η^{e1}	0.124	0.346	-0.009	0.639
y_η^{e2}	-0.253	0.389	0.154	0.152
$y_\eta^{\mu 1}$	0.746	0.220	-0.313	0.031
$y_\eta^{\mu 2}$	-0.307	-0.272	0.312	-0.440
$y_\eta^{\tau 1}$	0.705	-0.335	-0.400	-0.183
$y_\eta^{\tau 2}$	0.207	0.225	0.043	0.475
$\text{BR}(\mu \rightarrow e\gamma)$	2.730×10^{-13}	9.170×10^{-14}	1.428×10^{-13}	3.452×10^{-13}
$\text{BR}(\mu \rightarrow eee)$	3.686×10^{-13}	1.933×10^{-13}	9.799×10^{-14}	6.997×10^{-13}
$\text{BR}(\mu - e, Au)$	2.392×10^{-15}	1.599×10^{-16}	2.816×10^{-16}	2.122×10^{-16}
m_{ee} [meV]	3.67	48.36	3.67	48.36